

LOW SPEED AERODYNAMIC ANALYSIS
OF THE NASA GA(W)-2 AIRFOIL

by

THOMAS JOSEPH COGAN
Aerospace Engineering Department

Submitted in Partial Fulfillment of the Requirements of the
University Undergraduate Fellows Program

1976 - 1977

Approved by:

Balusu M. Rao
Dr. Balusu M. Rao
Faculty Advisor

May 1977

ABSTRACT

A recent development of the NASA Airfoil Research Program is a family of new high lift, low drag airfoils for application on general aviation aircraft. This study analyzes one of these airfoils, the 13% thick GA(W)-2, as to its lift, drag, and pitching moment characteristics, and compares it to airfoils used on current production aircraft. The analysis includes the results of two-dimensional wind tunnel tests as well as theoretical calculations made using thin airfoil theory and a lifting surface method.

ACKNOWLEDGMENTS

I would like to extend my sincere thanks to all those people who aided me in this research project for their advise, criticism, and encouragement. I would like to especially thank my advisor, Dr. Balusu M. Rao, and J. Rodney Matte, a graduate student in the Aerospace Engineering Department who helped in setting up the experimental equipment.

TABLE OF CONTENTS

	Page
Abstract	i
Acknowledgments	ii
List of Figures	iv
Introduction	1
Method	4
Theoretical Calculations	6
Discussion of Results	12
Bibliography	16
Table I	18
Table II	19
Table III	20
Figures	21
Vita	37

LIST OF FIGURES

Figure	Title	Page
1	Section profile of the NASA GA(W)-2 airfoil.	21
2	Chordwise pressure distribution around the GA(W)-2 airfoil for different angles of attack.	22
3	A comparison of the NACA 23015 and GA(W)-2 pressure distributions.	29
4	A comparison of the GA(W)-2 and NACA 23015 lift and pitching moment coefficients.	31
5	A comparison of the GA(W)-2 and NACA 23015 drag polars.	32
6	A comparison of the experimental lift and pitching moment coefficients with theory.	33
7	A comparison of experimental results with those obtained by NASA.	34
8	A comparison of experimental results obtained by NASA with those of three currently used NACA airfoils.	35

INTRODUCTION

On March 3, 1915, the Congress of the United States passed an act establishing the National Advisory Committee for Aeronautics (NACA), a conference committee whose function would be to encourage and supervise studies relating to the problems of flight. One of the goals set by the committee was the prediction of aerodynamic characteristics of different airfoil sections and subsequent improvement of their design. This task was made easier when an important theoretical development in the early 1930's permitted the calculation of inviscid flow about arbitrary airfoil shapes. Using this new tool, NACA designed a family of subsonic airfoil sections with prescribed pressure gradients such that laminar flow was maintained throughout the flight conditions for which it was designed. The airfoils which were built and tested displayed unsurpassed lift/drag characteristics and by 1950 had become the primary airfoils used on general aviation aircraft.

During the next fifteen years, very little progress was made in the development of subsonic airfoils. In 1965, however, a renewal of interest was generated by the major breakthrough of Richard Whitcomb at NASA Langley Research Center. Using computer optimization techniques, he designed a supercritical airfoil section which would reduce drag and improve the efficiency of aircraft in transonic flight. Its success prompted Whitcomb to apply the same basic computer program to the development of a low speed airfoil for a twin-engine, propeller driven general aviation aircraft. The resulting airfoil was the 17%

The citations on the following pages follow the style of the AIAA Journal.

thick GA(W)-1 [General Aviation (Whitcomb) - number one airfoil]. Experimental data obtained by NASA on this airfoil showed an increase in maximum section lift coefficient of five to fifteen percent greater than those of the 12-percent-thick four and five digit and 65 series NACA airfoils. Their results were published in December 1973 (McGhee and Beasley, 1973).

The achievement of high performance with the GA(W)-1 airfoil resulted in the formation of the NASA Airfoil Research Program in the spring of 1973. The first of a family of airfoils of differing thickness and camber has been developed through the program and is designated the GA(W)-2 (Figure 1). This 13-percent-thick airfoil was derived from the GA(W)-1 by linearly decreasing the mean thickness distribution of the GA(W)-1 and applying the thickness distribution to its mean camber line. Early indications (McGhee, et al, 1977) are that the GA(W)-2 is capable of obtaining a maximum section lift coefficient of up to 10 percent greater than that of the GA(W)-1 and 24 percent greater than those of the 12-percent-thick NACA sections. Extensive testing, however, will be required to evaluate its potential for use on general aviation aircraft.

The analysis of the GA(W)-2 airfoil presented in this paper is divided into two parts, an experimental and a theoretical. For the experimental portion, a two-dimensional model was constructed for testing in a 2 X 3 foot closed circuit wind tunnel. Tests included gathering data on the pressure distribution around the airfoil and graphically integrating it to find the lift and pitching moment coefficients, as well as running a pitot wake traverse for determining the drag coefficient. Experimental comparisons were made by running similar wind

tunnel tests on a NACA 23015 airfoil model and determining its lift, drag, and pitching moment coefficients. The second portion of the analysis, the theoretical, calculates the lift and pitching moment coefficients using both the conventional thin airfoil theory and a lifting surface method (Rao and Jones, 1973).

METHOD

The two-dimensional wind tunnel model of the 13-percent-thick GA(W)-2 airfoil was constructed using coordinates given in the NASA TM X-72697 (McGhee. et al, 1977) and listed in Table I. NASA obtained these coordinates by linearly decreasing the mean thickness distribution of the 17-percent-thick GA(W)-1 airfoil and applying this thickness distribution to its mean camber line. The resulting shape was predicted to have similar characteristics to the GA(W)-1 according to a theoretical analysis by NASA.

The airfoil model was constructed using a brass center section sandwiched between two sections of honduras mahogany shaped to the contour of the GA(W)-2. The total chord of the model was 30 cm with a span of 61 cm. Nineteen pressure orifices of 1 mm diameter were strategically located on both the upper and lower surfaces around the metal mid-section so as to enable an accurate measurement of the pressure distribution. The orifice locations are given in Table II. After final sanding of the model with number 400 wet-dry sandpaper, the two wood sections were sealed with a coat of spar varnish.

The model was mounted and tested in the 2 X 3 foot low speed closed circuit wind tunnel at Texas A&M University. This tunnel allows for a maximum unit Reynolds number of 1.58×10^6 per meter at a Mach number of 0.07. The model extended from one tunnel wall to the other with a minimum clearance at either end to ensure two-dimensional flow yet allow ease of rotation for the model. The angle of attack was set using a locking pin mechanism which permitted changing the angle of

attack in 2.5° increments through a range of -10° to 15° .

Measurement of the static pressures on the surface was accomplished using a single-step scanning valve system connected to a precision pressure transducer. The output from the transducer was fed into an OSC carrier amplifier and x-y plotter. The x-y plotter provided a hard copy of the pressure distribution, and thus a means for graphical integration to obtain section lift and pitching moment coefficients.

The sectional drag coefficient was experimentally calculated by using a wake traverse kiel probe to measure the variation in dynamic pressure behind the airfoil. From the dynamic pressure distribution, a velocity profile was determined and the change in momentum calculated. The section drag coefficient was then found by considering this change in momentum of the fluid across the airfoil.

The airfoil models, the GA(W)-2 and the NACA 23015, were tested at the maximum Reynolds number in order to obtain results with reasonable value. The angle of attack was varied from -10° to 10° in 5° increments and from 10° to 15° in 2.5° increments. The total and static pressures were measured for each run using a pitot static tube mounted about one chord's length in front of the model and connected to a precision micrometer.

THEORETICAL CALCULATIONS

Thin Airfoil Theory

This is an approximate method of analysis for finding the theoretical lifting characteristics of an arbitrary airfoil. In order to utilize the theory, certain conditions regarding the geometry of the airfoil must be met. It must have a small thickness to chord ratio, a small mean camber, and be moving through the fluid at a small angle of attack. These are not gross assumptions as they are usually fulfilled in the normal operation of conventional airfoils. The theory is based on replacing the airfoil with its mean camber line and neglecting viscous effects. The central problem becomes that of finding a vorticity distribution (γ) such that there be no pressure discontinuity at the trailing edge (Kutta condition) and that there be no flow through the surface. These boundary conditions at the airfoil can be written in the equation (Kuethe and Schetzer, 1959)

$$\frac{1}{2\pi} \int_0^c \frac{\gamma dx}{x_0 - x} = U_\infty \left(\alpha - \frac{dz}{dx} \right) \quad (1)$$

where α is the angle of attack, $\frac{dz}{dx}$ is the slope of the mean camber line at some point x , U_∞ is the free stream velocity, and c is the chord of the airfoil. The lift per unit span per unit chordwise distance is given by

$$p = \rho U_\infty \gamma \quad (2)$$

where p is the pressure differential acting on the airfoil. By integrating this over the chord, we find the lift per unit span.

$$L' = \int_0^c \rho p dx \quad (3)$$

The sectional lift coefficient, c_l , is given as

$$c_l = \frac{L'}{\frac{1}{2} \rho U_\infty^2 c} \quad (4)$$

Likewise, the moment of the lift about the leading edge of the airfoil is

$$M'_{LE} = -\int_0^c p x dx \quad (5)$$

and

$$c_{mLE} = \frac{M'_{LE}}{\frac{1}{2} \rho U_\infty^2 c^2} \quad (6)$$

The γ distribution may be written as a Fourier Series with arbitrary coefficients, $\{A\}$. The equation is

$$\gamma = 2U_\infty \left[A_0 \frac{1+\cos\theta}{\sin\theta} + \sum_{n=1}^{\infty} A_n \sin n\theta \right] \quad (7)$$

where θ is an independent variable found through a change of coordinate systems. The value of θ may be calculated as

$$\theta = \cos^{-1} \left(1 - \frac{2x}{c} \right) \quad (8)$$

Substituting equation 7 into equation 1 and simplifying, the resulting equation becomes

$$\frac{dz}{dx} = (\alpha - A_0) + \sum_{n=1}^{\infty} A_n \cos n\theta \quad (9)$$

From this we can write

$$A_0 = \alpha - \frac{1}{\pi} \int_0^{\pi} \frac{dz}{dx} d\theta \quad (10)$$

$$A_n = \frac{2}{\pi} \int_0^{\pi} \frac{dz}{dx} \cos n\theta d\theta \quad (11)$$

By substituting equations 10 and 11 into equation 7, the lift and pitching moment can be derived to be

$$c_l = 2\pi A_0 + \pi A_1 \quad (12)$$

$$c_{m_{LE}} = -\frac{c_l}{4} + \frac{\pi}{4} (A_2 - A_1) \quad (13)$$

By dividing the moment about the leading edge by the lift, we find that the center of pressure is at the 25 percent chord and the pitching moment coefficient at that point is independent of angle of attack.

It has the value

$$c_{m_{c/4}} = \frac{\pi}{4} (A_2 - A_1) \quad (14)$$

Numerical Lifting Surface Method

The basic theory and procedure for this method (Rao and Jones, 1973) replaces the airfoil with an appropriate vortex (doublet) distribution, the strength of which is such that the tangential flow condition over the solid boundary and the Kutta condition are satisfied. The governing flow equation relating the downwash at any point p on the surface to the doublet distribution on the surface and wake is given by

$$2\pi W_p = \int_s k \frac{\partial}{\partial x} \left(\frac{1}{x - x_p} \right) dx \quad (15)$$

where $k = \phi_u - \phi_l$ (discontinuity in velocity potential)

and s is the airfoil surface and its wake. In the numerical procedure adopted, the airfoil surface is divided up into a number of finite strips (N) over which k is assumed to be constant. The k in the wake is related to the k of the trailing edge strip through the Kutta condition ($k_{\text{wake}} = k_N$).

A non-dimensional procedure is then used to replace k with KUc' and x with Xc' , where U is the free stream velocity and c' is the semi-chord. Equation 15 becomes

$$2\pi \left(\frac{W}{U} \right)_p = \int_{-1}^{\infty} K \frac{\partial}{\partial X} \left(\frac{1}{X - X_p} \right) dX \quad (16)$$

Written in numerical form

$$2\pi \left\{ \frac{W}{U} \right\}_i = [A] \{K\} \quad i = 1, 2, 3, \dots, N \quad (17)$$

where

$$\left\{ \frac{W}{U} \right\}_i = \alpha_i - \left(\frac{dz}{dx} \right)_i$$

$$a_{in} = \frac{1}{X_n + D_n - X_i} - \frac{1}{X_n - D_n - X_i} \quad \text{for } n \neq N$$

and

$$a_{in} = \frac{1}{X_i + D_n - X_n} \quad \text{for } n = N$$

where $2D_n$ is the width of the n th strip.

The matrix $[A]$ in equation 17 may be considered as an aerodynamic influence coefficient matrix. The product $a_{in} K_n$ represents the velocity induced at the i th point on the airfoil surface by the K_n distribution at the n th strip. As can be seen, the problem is reduced to that of solving a set of linear algebraic equations for a given set of flow conditions. Once the K distribution is obtained, the lift and moment coefficients can be found. Remembering that c_l is

$$\begin{aligned} c_l &= \frac{L'}{\frac{1}{2} \rho U^2 c} \\ &= \frac{2L'}{\rho U^2 c} \end{aligned}$$

and since

$$\begin{aligned} L' &= \rho U k_{te} \\ &= \rho U^2 c K_{te} \\ &= \rho U^2 c K_N \end{aligned}$$

the lift coefficient is found to be

$$c_l = 2K_N$$

The pitching moment can be expressed as

$$\begin{aligned} M &= -\rho U^2 (c')^2 \int_{-1}^1 \frac{\partial K}{\partial X} (X - x_p) dX \\ &= -\rho U^2 (c')^2 \left[K_N (1 - x_p) - \int_{-1}^1 K dX \right] \end{aligned}$$

Since c_m is given as

$$\begin{aligned} c_m &= \frac{M}{\frac{1}{2} \rho U^2 (c')^2} \\ &= \frac{2M}{\rho U^2 (c')^2} \end{aligned}$$

we find the moment coefficient to be

$$\begin{aligned} c_m &= -2 \left[K_N (1 - x_p) - \int_{-1}^1 K dX \right] \\ &= -2 \left[K_N (1 - x_p) - \sum_{n=1}^N K_n \Delta X_n \right] \end{aligned}$$

DISCUSSION OF RESULTS

Pressure Distribution

Important to the aerodynamic characteristics of the NASA GA(W)-2 is the pressure distribution around the airfoil at various angles of attack. Figure 2 contains graphs of this pressure distribution for all the angles of attack at which the airfoil was tested. Of particular significance is the relatively small pressure gradient along the upper surface of the GA(W)-2, as can be seen by comparison with the pressure distribution of the conventional NACA 23015 airfoil at an angle of attack of five degrees (Figure 3). It is this smaller pressure gradient that results in the good stall characteristics of the GA(W)-2.

Stall, or loss of lift, occurs when the flow over the upper surface of the airfoil becomes detached or separated. This phenomena is brought about when the air particles flowing across the upper surface of the airfoil lose sufficient kinetic energy to overcome the adverse pressure gradient, and hence begin flowing in the opposite direction as the free stream. The presence of a small pressure gradient aft of the point of maximum velocity on the upper surface allows the particles to travel further along the surface before losing their momentum, resulting in delayed flow separation and stall.

Lift

The upper portion of the graph in Figure 4 gives a comparison of the experimentally determined lift coefficients versus angle of attack for the GA(W)-2 and NACA 23015 airfoils at a Reynolds number of 4.74×10^5 . For any given angle of attack up to the point of stall, the GA(W)-2

exhibits a higher lift coefficient than the NACA 23015, and exhibits a higher lift curve slope at the angles of attack within the normal flight regime. However, unlike the results obtained by NASA, both airfoils had the same maximum coefficient of lift, 1.3.

Another point of interest illustrated by the graph in Figure 4 is the stall characteristics of these airfoils. There exists a high degree of linearity in the lift curve slope of the NACA 23015 airfoil up to an angle of attack of about twelve or thirteen degrees, at which point it stalls abruptly. The GA(W)-2 on the other hand begins to show signs of flow separation at about five degrees angle of attack with complete separation occurring at twelve to thirteen degrees. The significance here, attributable to the small pressure gradient on the GA(W)-2, is that the more gentle stall characteristics are a very desirable condition for general aviation aircraft application.

Table III contains a comparison of the lift and pitching moment coefficients for the GA(W)-2 as determined using thin airfoil theory and the lifting surface method. As is shown in Table III and by examination of the graph in Figure 6, both methods of calculation are in close agreement as to the lift curve slope and coefficient of lift at small angles of attack. However, since neither of the theories predict stall, the close agreement between the experimental values and the theoretically calculated values ends at higher angles of attack. The lift curve slope found experimentally was 0.108 per radian, essentially the best possible according to thin airfoil theory. The lifting surface theory, on the other hand, exhibits a value slightly less than ideal.

The experimental results obtained by NASA are compared to those obtained through this project in Figure 7. The lift curve slope of the

former is slightly greater than that of the latter, and slightly greater than what is predicted by theory. At a Reynolds number of 2.1×10^6 , NASA was able to obtain a maximum section lift coefficient of over 1.6. The limitations of the wind tunnel used in this project prevented duplicating these results. At the lower Reynolds number of 4.74×10^5 , the maximum lift coefficient obtained was 1.3, and the airfoil stalled at a lower angle of attack. According to trends of the effect of Reynolds number on the maximum lift coefficient (Abbott and Von Doenhoff, 1967), this value seems reasonable.

Figure 8 is a comparison of the results found by NASA in testing the GA(W)-2 with those of three currently used NACA airfoil sections. As indicated by the figure, the GA(W)-2 exhibits a substantially greater lift curve slope than the NACA 4412 and 65₁-412 airfoils, and exhibits a maximum section lift coefficient greater than all three.

Pitching Moment

According to thin airfoil theory, the pitching moment about the quarter chord point (center of pressure) is constant and equal to $-.117$. Lifting surface theory calculates it to be linearly decreasing with increasing angle of attack. The two theories are compared with the experimental results in Figure 6. As can be seen, the experimental results are not constant, nor are they of as great a magnitude as predicted by the theories. As the wing stalls, there is a very abrupt increase in the pitching moment coefficient as would be expected.

Figures 4 and 8 indicate that the pitching moment coefficient of the GA(W)-2 is substantially greater than the NACA five digit series airfoils and slightly greater than the NACA 4412 and 65₁-412 airfoils.

Though a smaller pitching moment coefficient is more desirable, the effect of a larger pitching moment coefficient can be negated in the design of the aircraft on which the airfoil is to be used.

Drag

Figure 5 gives a comparison of the experimentally determined drag polars for the GA(W)-2 and NACA 23015 airfoils at a Reynolds number of 4.74×10^5 . At the section lift coefficients within the range of the normal flight regime, the GA(W)-2 exhibits a lift-to-drag ratio of ten percent better than the 23015. This is a substantial increase and indicates that the GA(W)-2 is indeed a more efficient airfoil.

Figure 8 shows the drag polar obtained by NASA through their tests on the GA(W)-2 (McGhee, et al, 1977) and compares it to the NACA 12-percent-thick sections. At this Reynolds number, 6.0×10^6 , it also shows an increase in lift-to-drag ratio over the NACA airfoils.

Bibliography

1. Abbott, Ira H. and Albert E. Von Doenhoff, Theory of Wing Sections, Dover Publications, Inc., New York, 1967.
2. Dommasch, Daniel O., Sydney S. Sherby, and Thomas Connally, Airplane Aerodynamics, Pitman Publishing Company, New York, 1967.
3. Kocivar, Ben, "NASA's Super Wing Gives New Lift to Small Planes", Popular Science Magazine, April 1975, Times Mirror Magazines, New York, pp. 78-80, 134,136.
4. Kuethe, A. M. and J. D. Schetzer, Foundations of Aerodynamics, John Wiley & Sons, Inc., New York, 1959.
5. McGhee, Robert J. and William D. Beasley, NASA TN D-7428 Low Speed Aerodynamic Characteristics of a 17-Percent-Thick Airfoil Section Designed for General Aviation Applications, December 1973.
6. McGhee, Robert J., William D. Beasley, and Dan M. Somers, NASA TM X-72697 Low Speed Aerodynamic Characteristics of a 13-Percent-Thick Airfoil Section Designed for General Aviation Application, For general release May 1977.
7. Pierpont, Kenneth, "Bringing Wings of Change", Aeronautics and Astronautics, October 1975, AIAA, New York, pp. 20-24.

8. Rao, B. M. and W. P. Jones, "Summary of the Results of a Simplified Aerodynamic Theory of Lifting Surfaces in Subsonic Flow", TEES-2600-TR-73-01, Texas A&M University, June 1973.

TABLE I
 NASA GA(W)-2 Airfoil Coordinates
 (c = 30 cm)

x/c	(z/c) _{upper}	(z/c) _{lower}	x/c	(z/c) _{upper}	(z/c) _{lower}
0.0	0.0	0.0	.54954	.08025	-.03803
.00199	.00922	-.00486	.57452	.07835	-.03582
.00498	.01481	-.00847	.59950	.07609	-.03326
.01246	.02365	-.01385	.62448	.07342	-.03048
.02498	.03304	-.01870	.64946	.07035	-.02745
.03747	.03957	-.02196	.67444	.06688	-.02428
.04996	.04460	-.02465	.69942	.06305	-.02107
.07494	.05230	-.02904	.72440	.05890	-.01783
.09992	.05831	-.03246	.74938	.05446	-.01460
.12490	.06323	-.03528	.77435	.04974	-.01145
.14988	.06731	-.03769	.79933	.04476	-.00851
.17485	.07080	-.03966	.82431	.03956	-.00587
.19983	.07381	-.04129	.84929	.03417	-.00357
.24980	.07857	-.04353	.87427	.02864	-.00187
.29975	.08171	-.04471	.89925	.02296	-.00086
.34971	.08357	-.04508	.92423	.01712	-.00052
.39967	.08441	-.04475	.94921	.01112	-.00143
.44963	.08425	-.04363	.97419	.00497	-.00377
.49958	.08294	-.04149	.99917	-.00143	-.00720
			1.0	-.00164	-.00732

TABLE II
GA(W)-2 Airfoil Orifice Locations
(c = 30 cm)

$(x/c)_{\text{upper}}$	$(x/c)_{\text{lower}}$
0.0	0.0
.010	.010
.023	.023
.040	.040
.063	.063
.093	.093
.130	.130
.173	.173
.223	.223
.280	.280
.340	.343
.403	.413
.467	.487
.530	.560
.593	.630
.657	.697
.720	.760
.783	.820
.850	.877
.917	.930

TABLE III

A Comparison of Thin Airfoil Theory and Lifting
Surface Theory Two-Dimensional Lift and Pitching Moment Coefficients

α (degrees)	Thin Airfoil Theory		Lifting Surface Theory	
	c_l	$c_{m_{c/4}}$	c_l	$c_{m_{c/4}}$
-8	-0.38561	-0.11718	-0.40285	-0.11937
-6	-0.18828	-0.11718	-0.18437	-0.11736
-4	0.05304	-0.11718	0.03410	-0.11534
-2	0.27237	-0.11718	0.25257	-0.11332
0	0.49169	-0.11718	0.47104	-0.11131
2	0.71101	-0.11718	0.68951	-0.10929
4	0.93034	-0.11718	0.90798	-0.10727
6	1.14966	-0.11718	1.12645	-0.10525
8	1.36899	-0.11718	1.34493	-0.10324
10	1.58831	-0.11718	1.56399	-0.10122
12	1.80764	-0.11718	1.78187	-0.09920
14	2.02696	-0.11718	2.00034	-0.09718
16	2.24628	-0.11718	2.21881	-0.09517
18	2.46561	-0.11718	2.43728	-0.09315
20	2.68493	-0.11718	2.65576	-0.09113

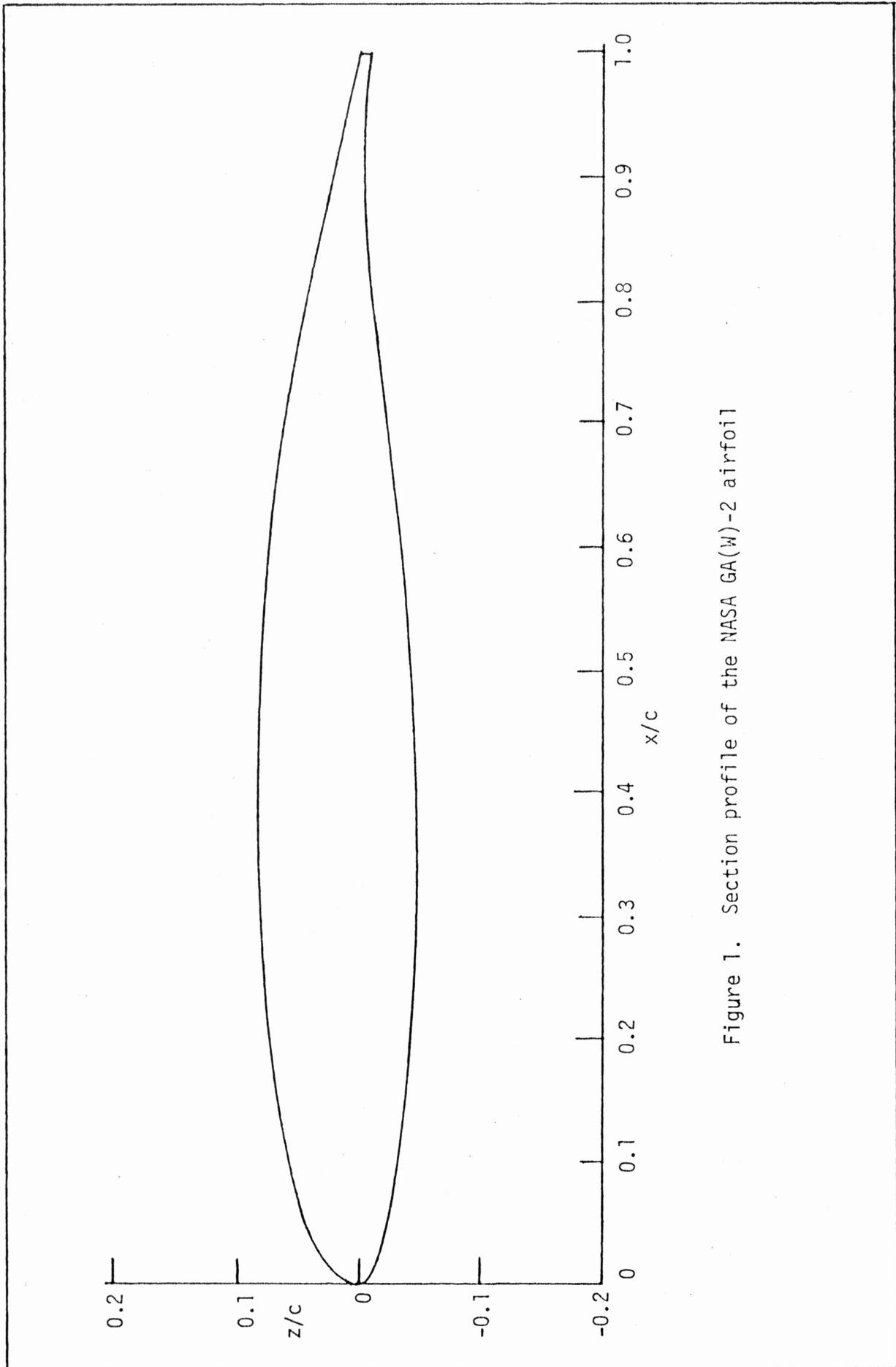


Figure 1. Section profile of the NASA GA(W)-2 airfoil

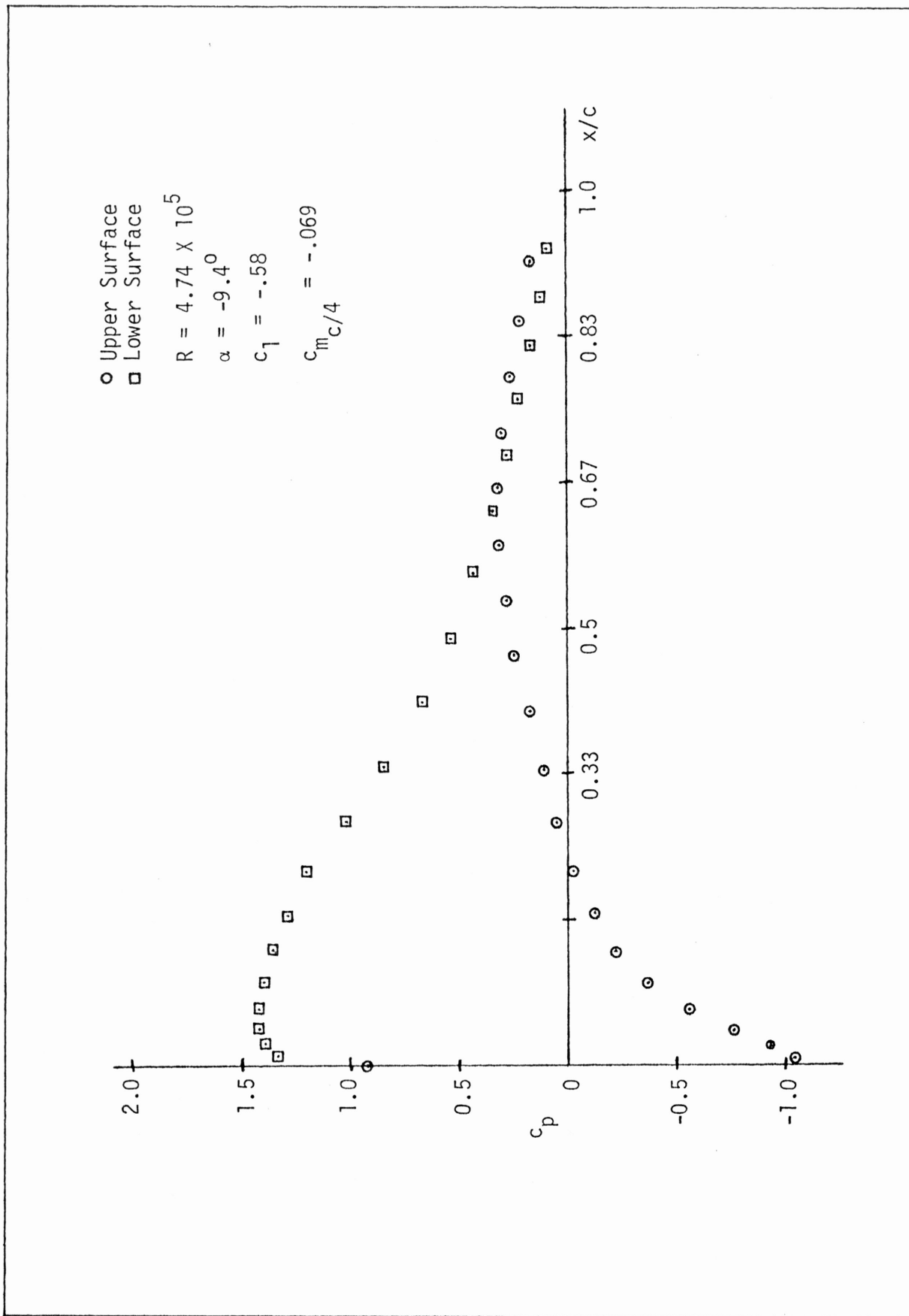


Figure 2. Chordwise pressure distribution around the GA(W)-2 airfoil for different angles of attack. (Flagged symbol indicates base orifice location).

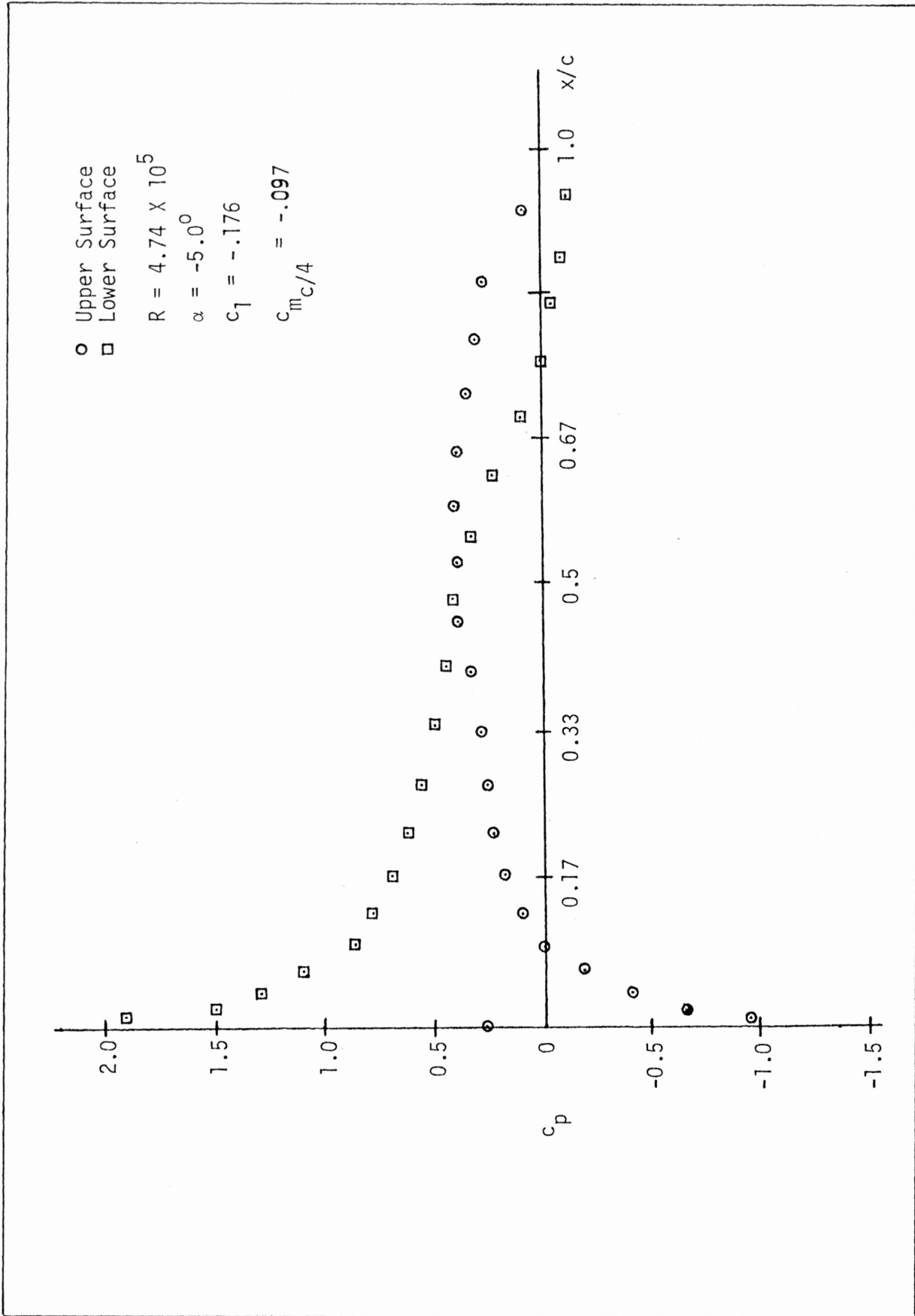


Figure 2. Continued

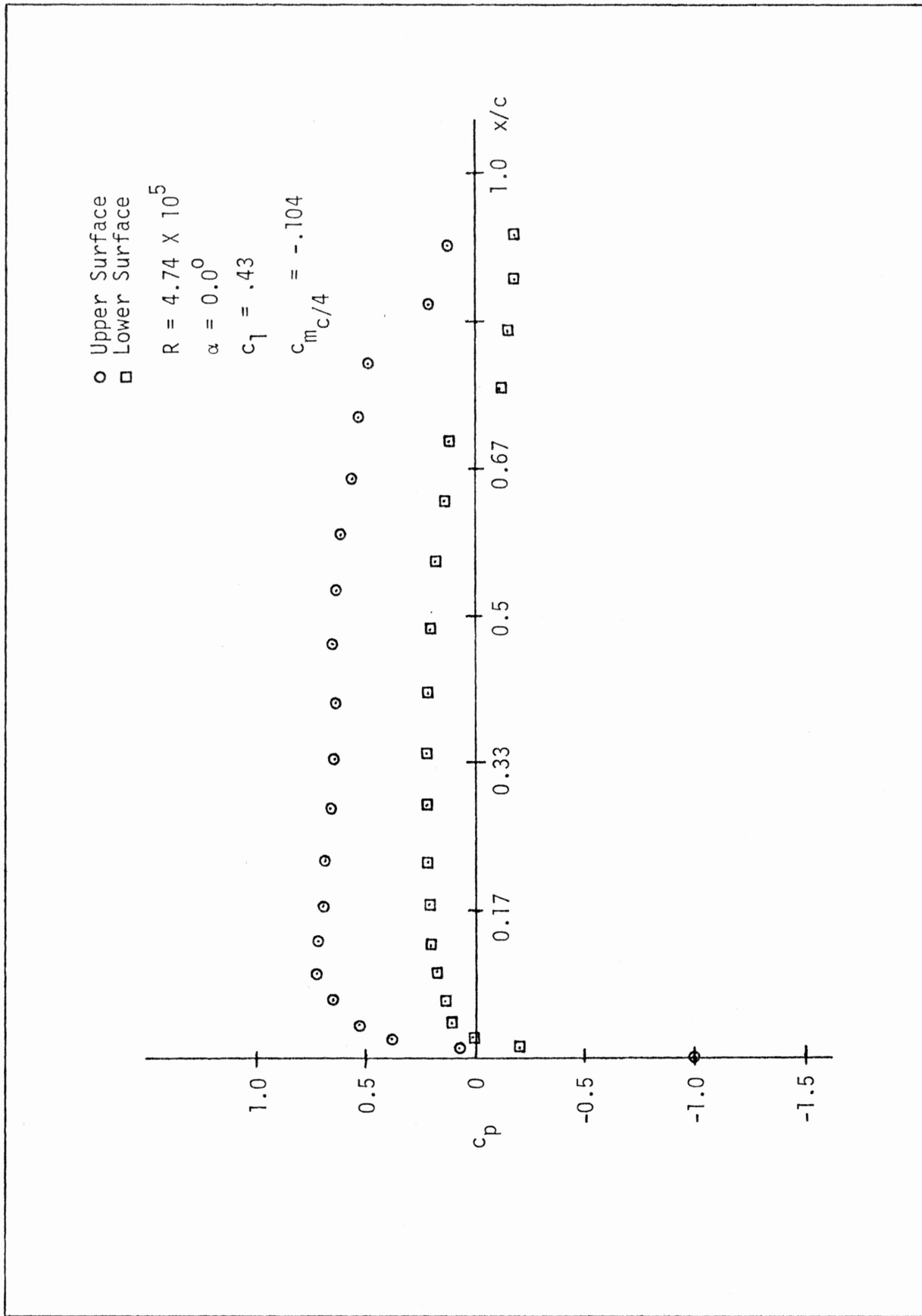


Figure 2. Continued

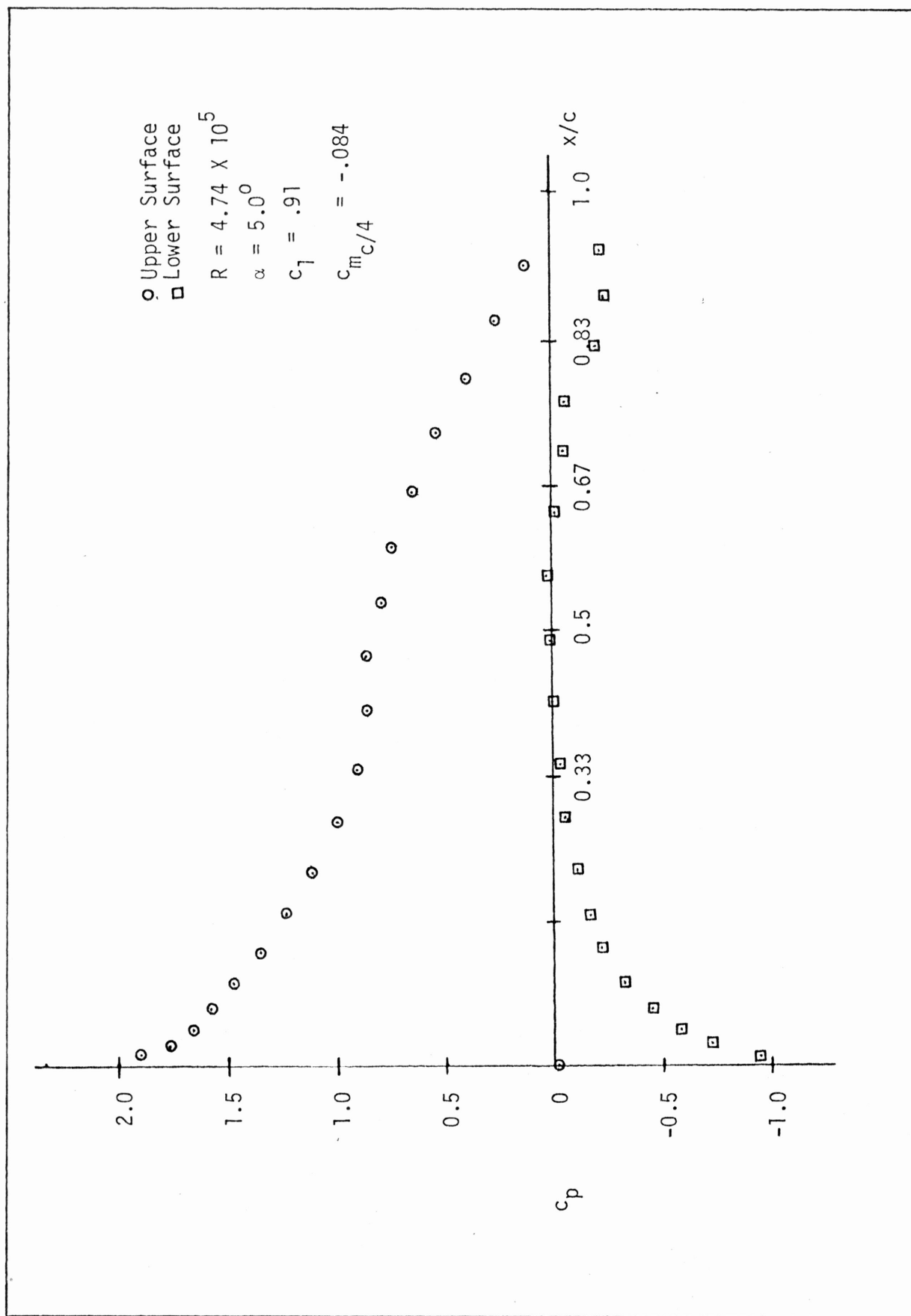


Figure 2. Continued

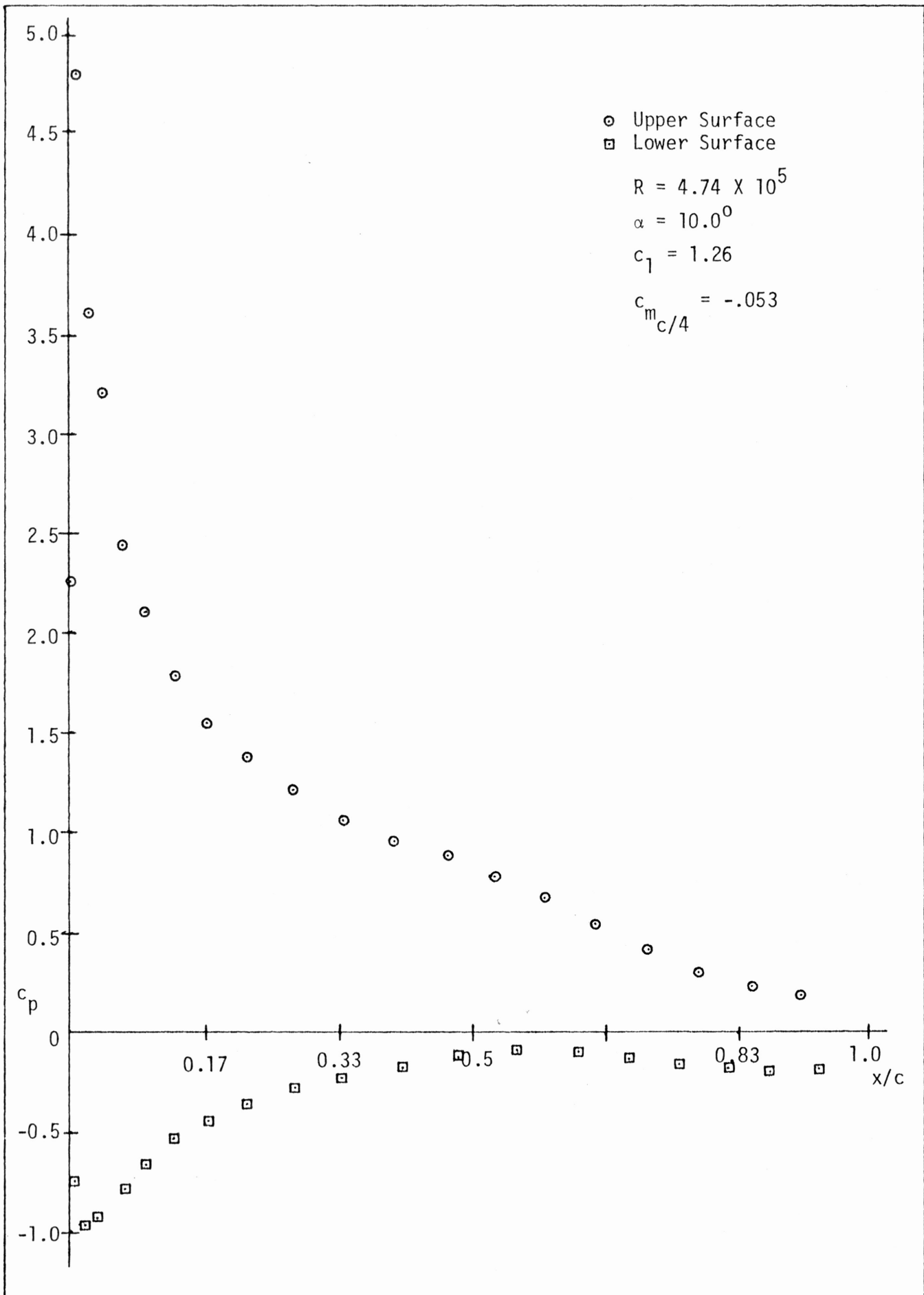


Figure 2. Continued

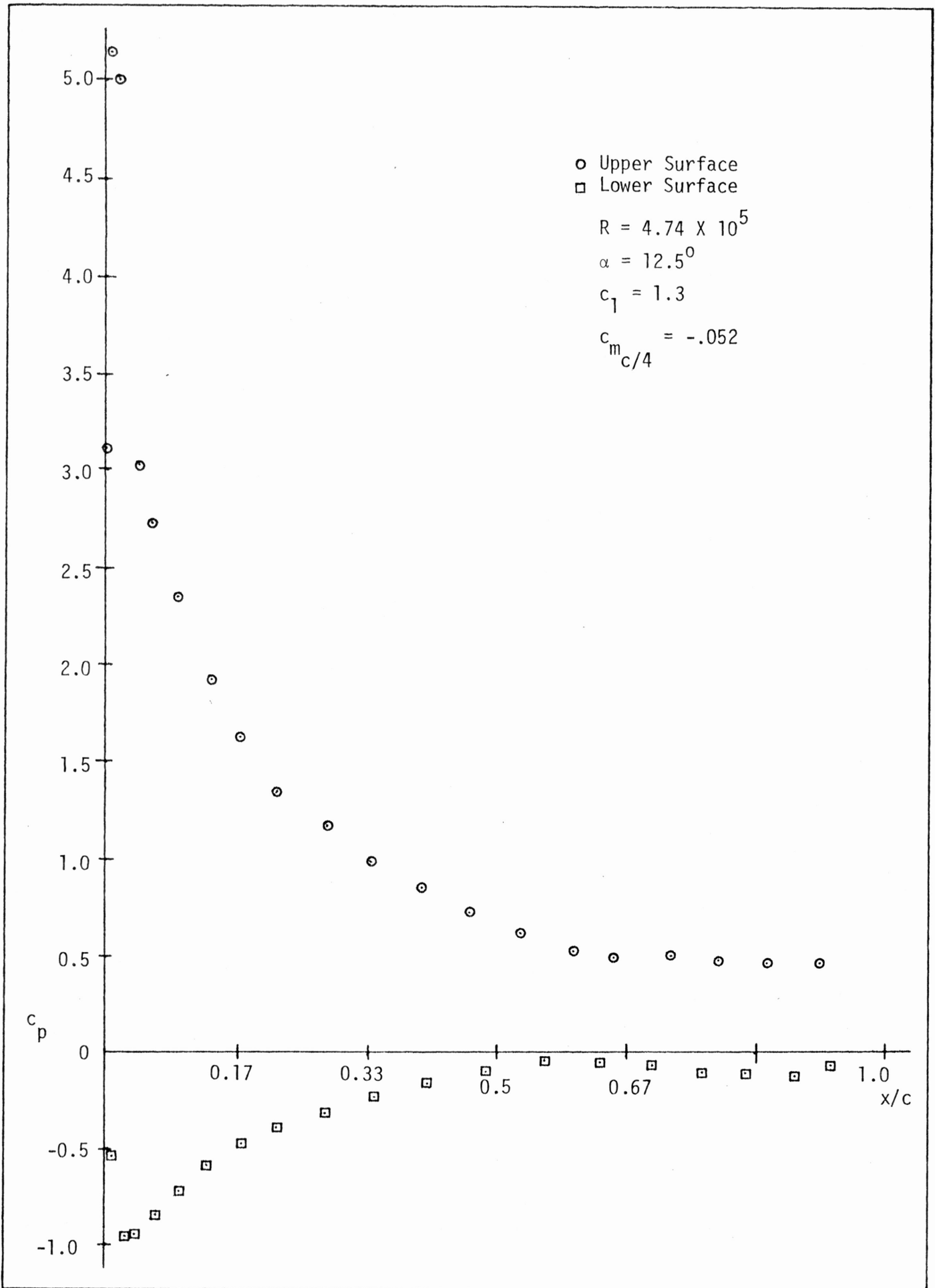


Figure 2. Continued

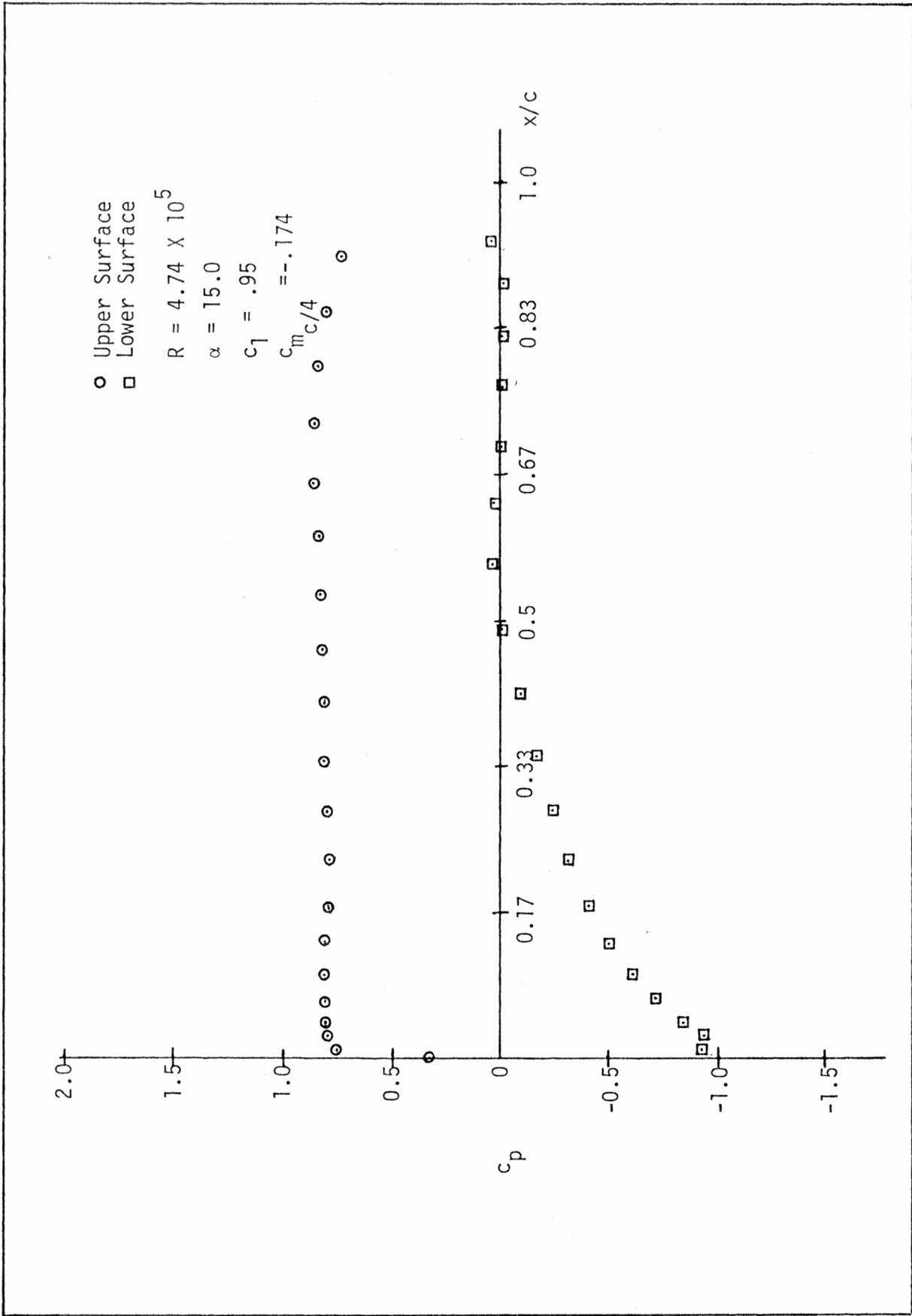


Figure 2. Concluded

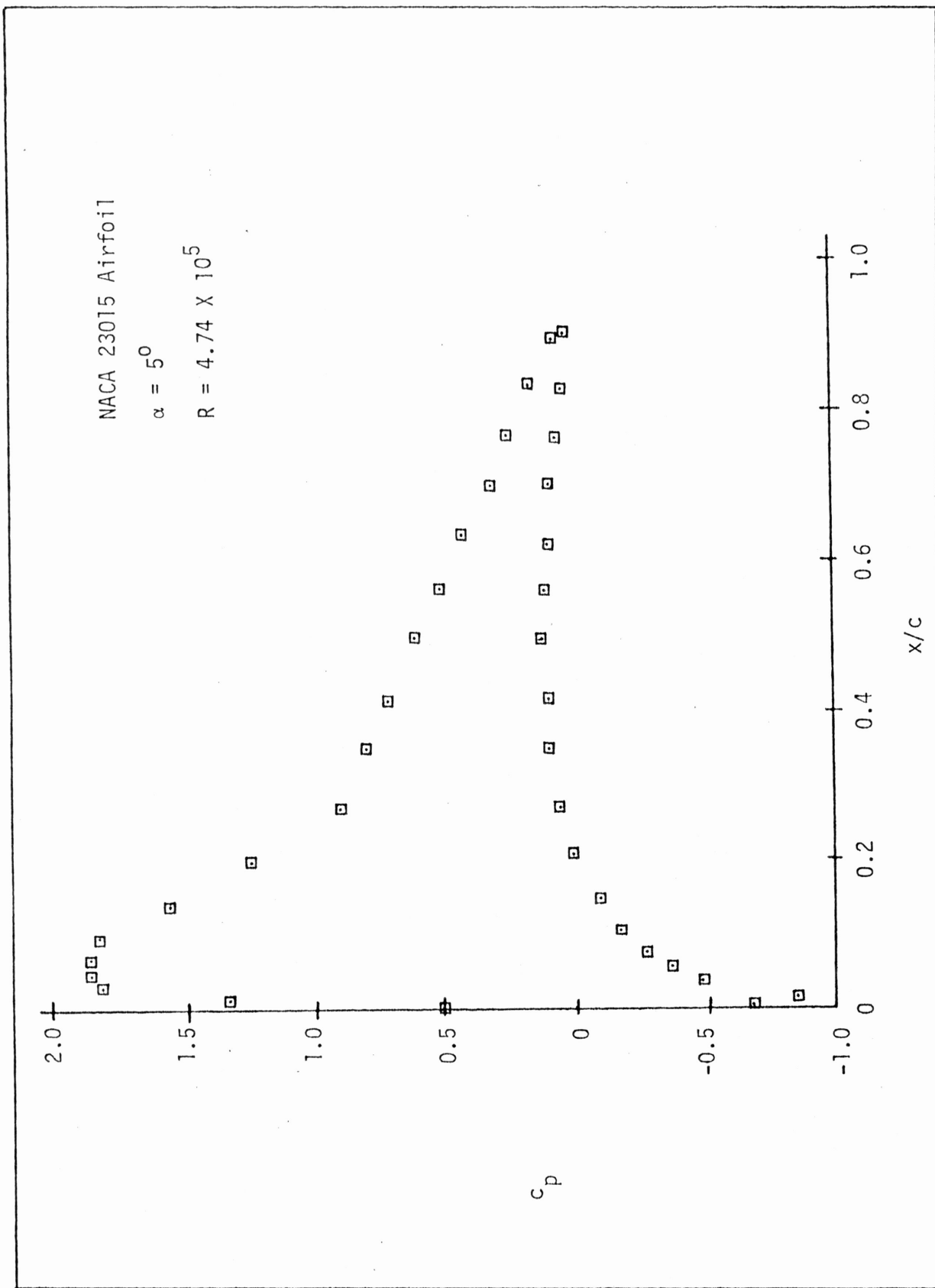


Figure 3. A comparison of the NACA 23015 and GA(W)-2 chordwise pressure distributions.

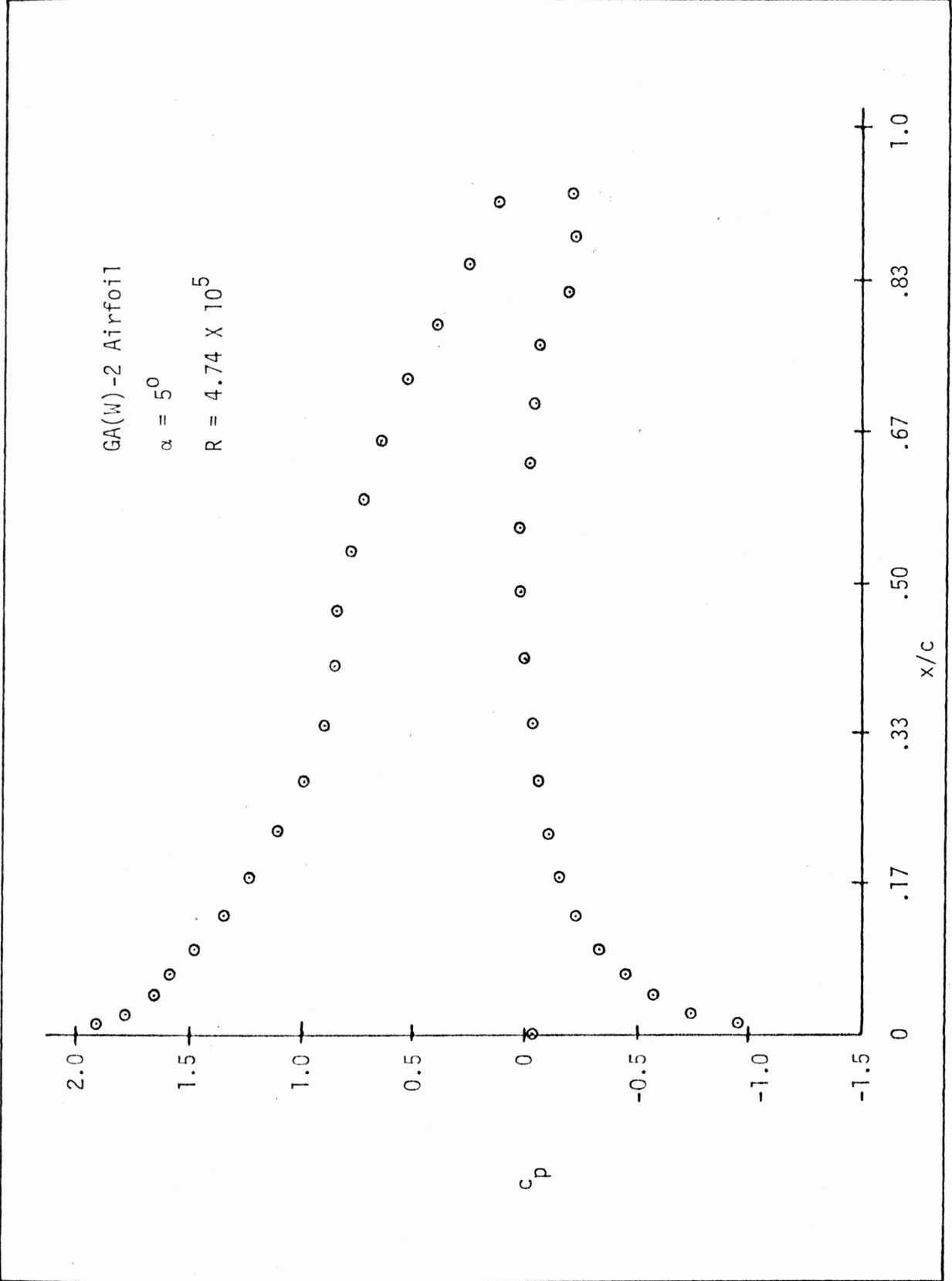


Figure 3. Concluded

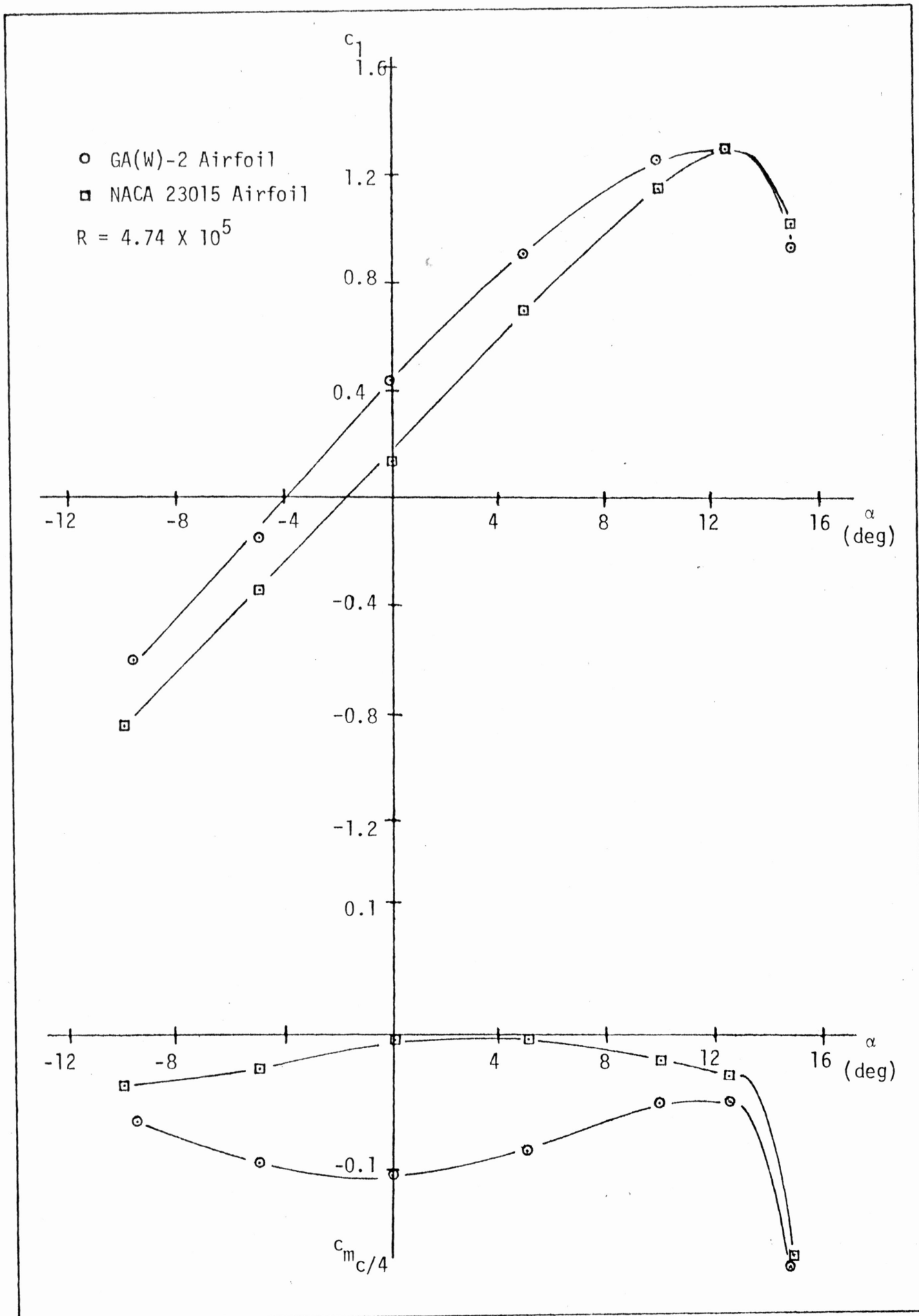


Figure 4. A comparison of the GA(W)-2 with the NACA 23015 airfoil.

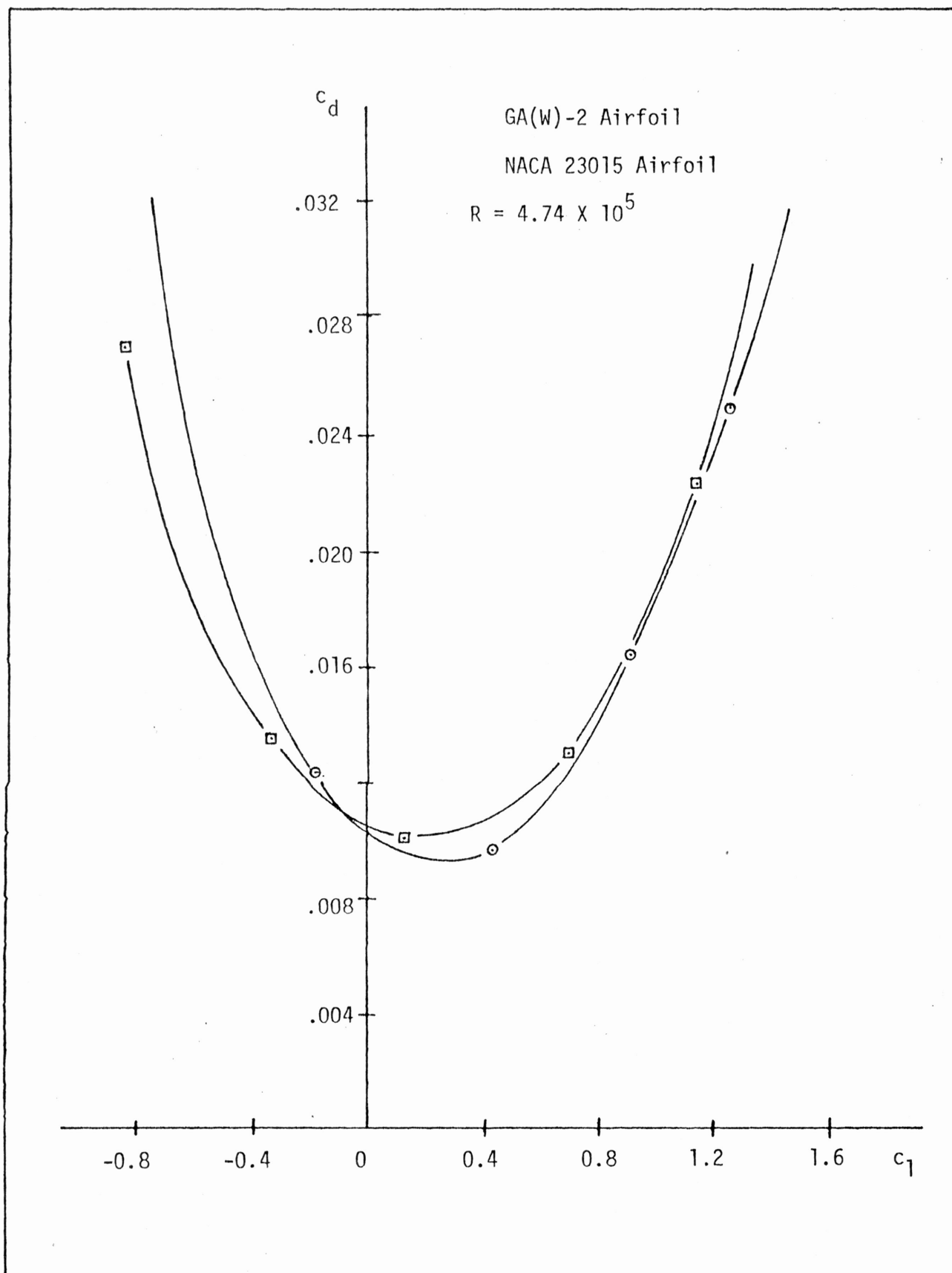


Figure 5.

A comparison of the GA(W)-2 and NACA 23015 drag polars.

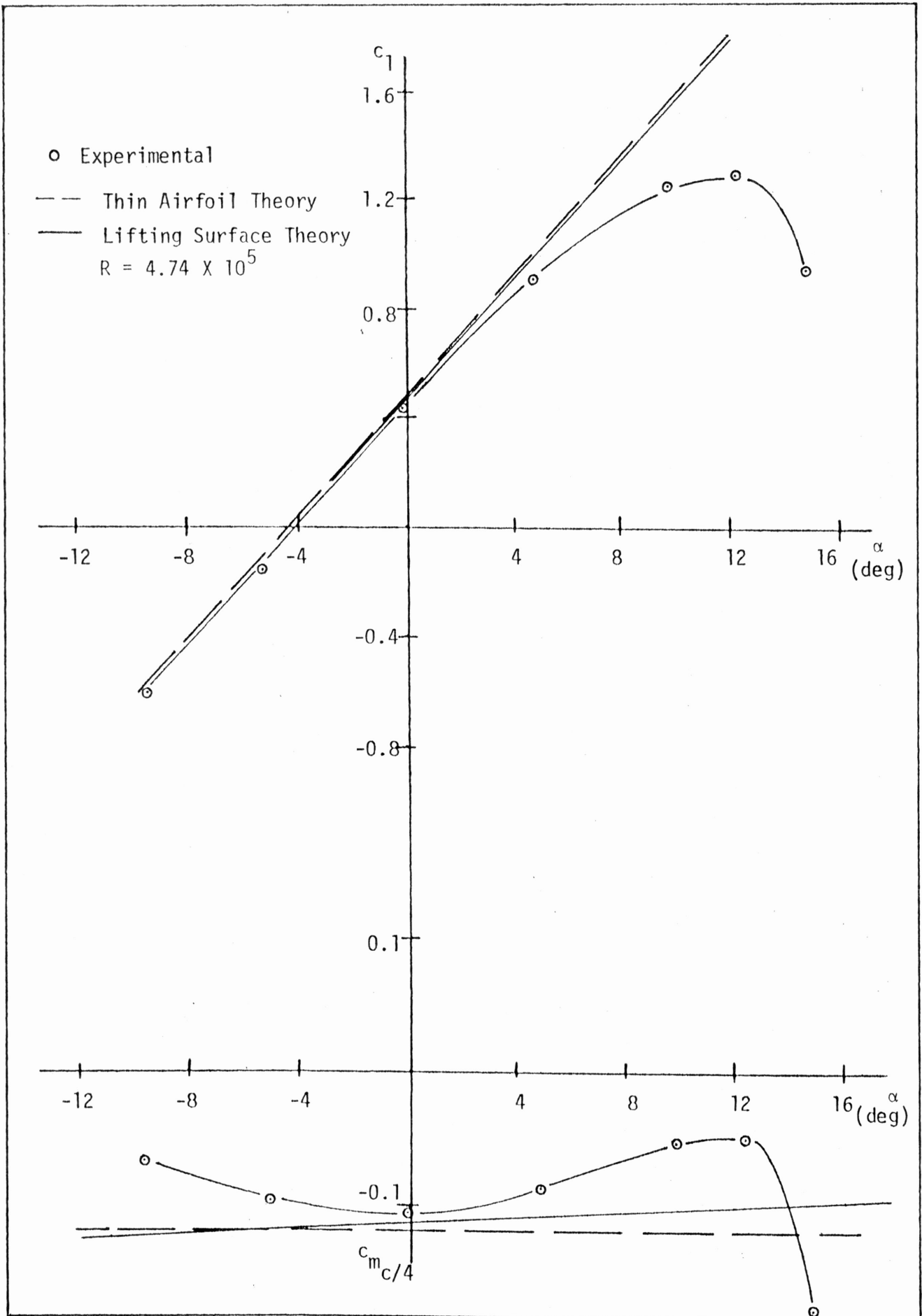


Figure 6. A comparison of experimental c_l and $c_{m_{c/4}}$ with theory.

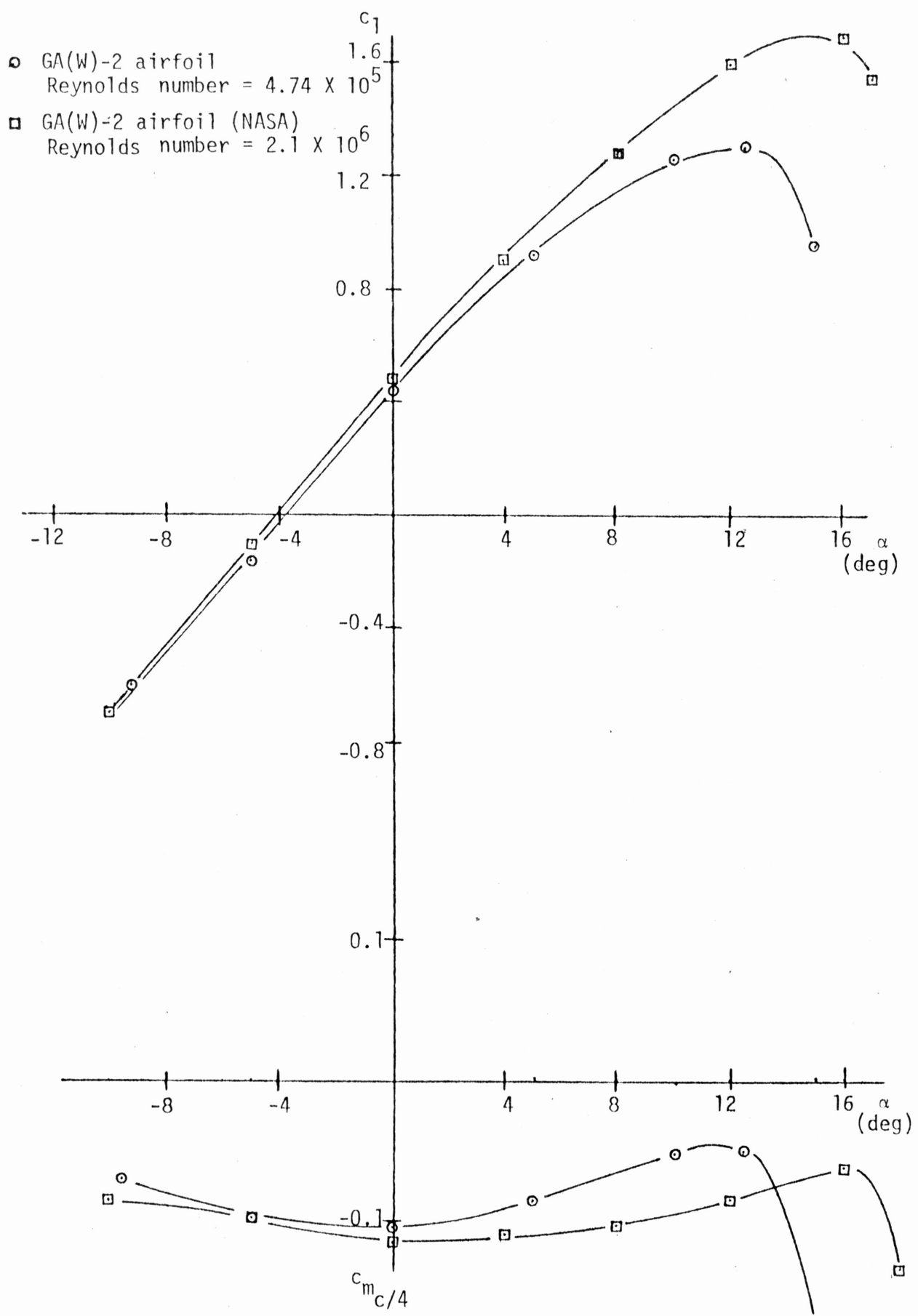


Figure 7. A comparison of results with those obtained by NASA.

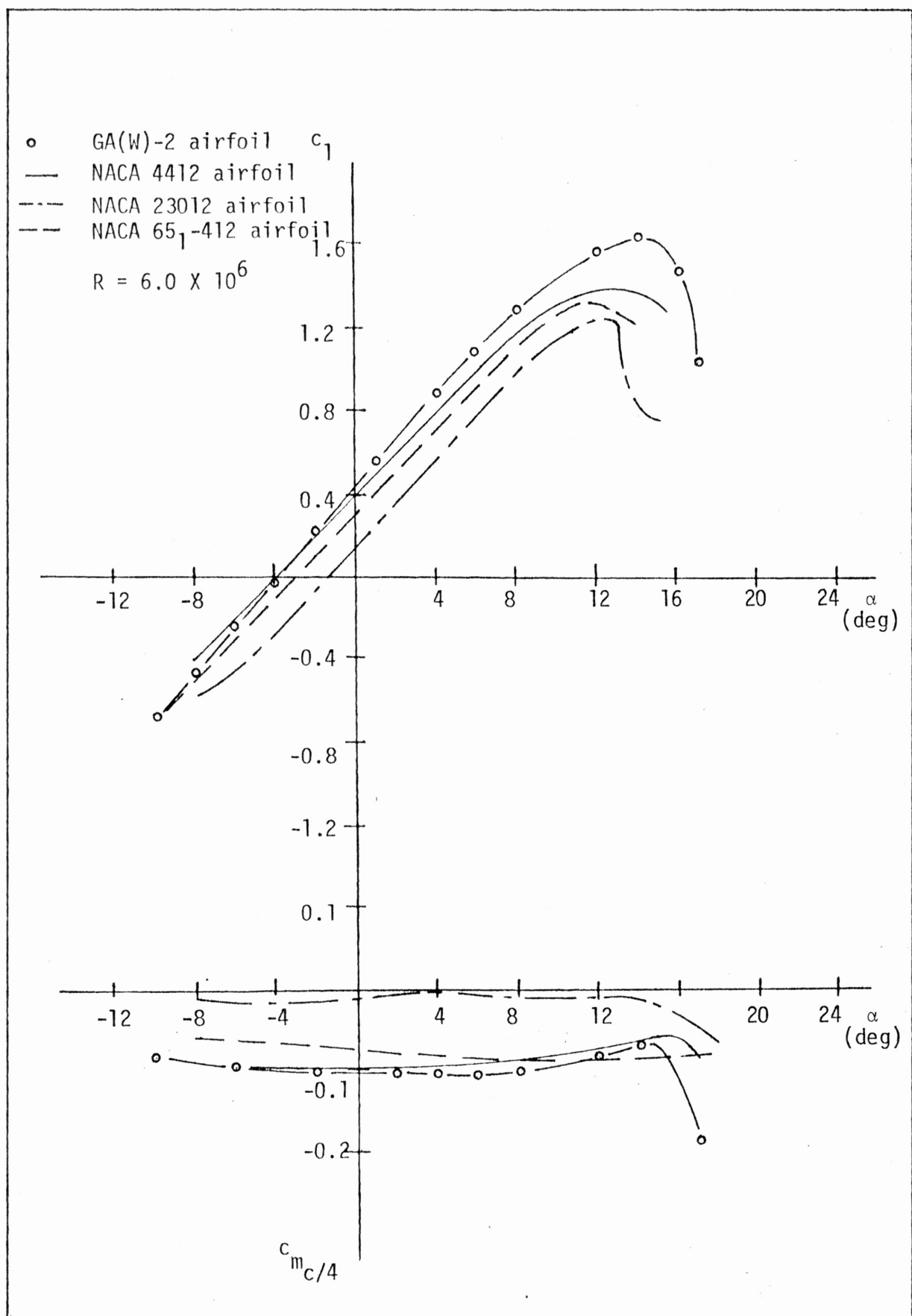


Figure 8. A comparison of experimental results obtained by NASA with those of three currently used NACA airfoils.

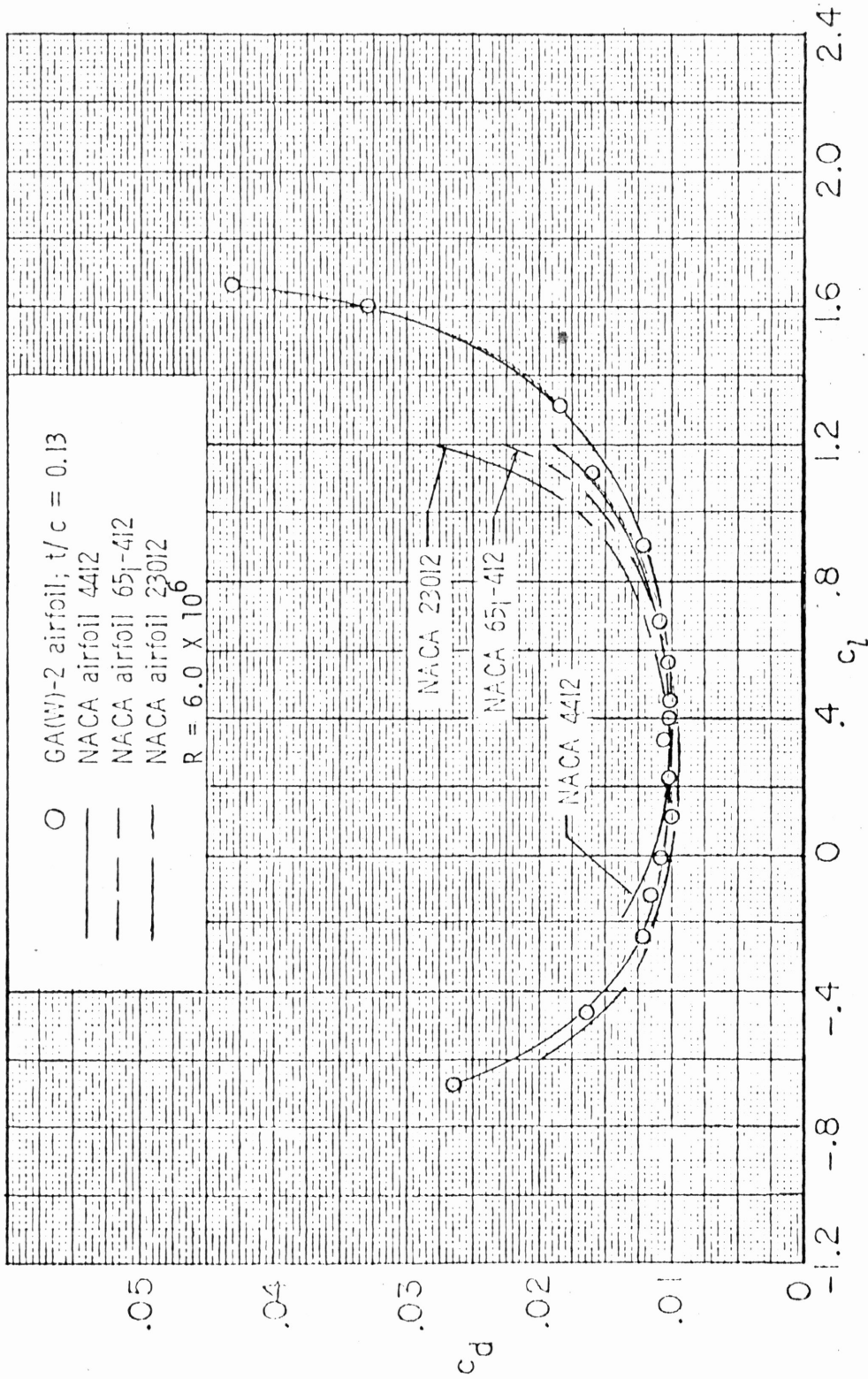


Figure 8. Concluded